Simulation of the Catalytic Cracking Process for Styrene Production

Abstract: A mathematical model is presented for simulating the steady-state catalytic dehydrogenation of ethylbenzene to styrene and other associated side reactions. The various differential equations describing the material and energy balances were integrated using a fourth-order Runge-Kutta method on an IBM 7090. Several runs on the computer were made to study the effect of change in feed rates, feed-to-steam ratio, and inlet temperature and pressure, on styrene yield. It is shown how, with the computer results, a profit equation for a particular plant may be derived for possible use in on-line optimization and control.

 n_{18}

Nomenclature

C_p^0	ideal gas heat capacity at constant pressure, cal/g-mole, °C
D	inside diameter of empty reactor, cm
F	g-moles of ethylbenzene in feed, moles/sec
ΔH_i^0	standard heat of reaction for i^{th} event, cal/g-mole
	, , ,
K_a	equilibrium constant for reaction (in terms of activities)
K_p	equilibrium constant for reaction (in terms of
p	partial pressures)
N_i	g-moles per sec of ith specie at equilibrium in
	reactor
N_s	g-moles of steam fed per second
n_9	g-moles of ethylbenzene at a point in the reactor
	per sec
n_{10}	g-moles of styrene at a point in the reactor per sec
n_{11}	g-moles of hydrogen at a point in the reactor per sec
n_{12}	g-moles of benzene at a point in the reactor per sec
n_{13}	g-moles of ethylene at a point in the reactor per sec
n_{14}	g-moles of toluene at a point in the reactor per sec
n_{15}	g-moles of methane at a point in the reactor per sec
n_{16}	g-moles of carbon monoxide at a point in the
	reactor per sec
n_{17}	g-moles of steam at a point in the reactor per sec

g-moles of carbon dioxide at a point in the reactor per sec g-moles of acetylene at a point in the reactor per sec

- p_i partial pressure of j^{th} species, atm
- r equal to N_s/F
- r_i reaction rate for the j^{th} specie, g-moles/sec \times cc or g-moles/sec \times g-catalyst
- R gas constant
- T temperature, °K
- U over-all heat transfer coefficient, cal/sec \times cm² °C
- V_R empty reactor volume, cc
- V_F free volume of the packed reactor, cc
- W mass of catalyst in reactor, gm
- X_i fractional conversion in the i^{th} reaction
- Y_i equilibrium fractional conversion for the $i^{
 m th}$ reaction
- z dimension along the bed depth, cm
- α cross-sectional area of empty reactor, cm²
- $\Delta \alpha$ constants in equations for heat capacity
- $\Delta\beta$ constants in equations for heat capacity
- $\Delta \gamma$ constants in equations for heat capacity
 - volume of catalyst pellets per volume of empty reactor
- π total pressure at any point in the reactor, atm
- π_0 pressure at reactor inlet, atm
- ρ_w particle density of catalyst in reactor, gm/cc

 n_{19} g-moles of acetylene at a point in the reactor per sec n_{20} g-moles of coke at a point in the reactor per sec n_t total g-moles of gas per sec in the reactor at a point

Present address: Rutgers, the State University, Department of Chemical Engineering, New Brunswick, N.J.

Introduction

Digital computer control in the chemical industry has gained considerable interest in recent years. Initial attempts toward closed-loop control with digital computers encountered some difficulties primarily due to inexperience, on the part of the computer industry, regarding the nature of chemical plant units. For example, it is now well recognized that a chemical reactor is not only nonlinear but also that its behavior cannot be expressed in the form of transfer functions or simple regression models, if one intends to utilize these relationships for reactor conditions other than those used for obtaining the models. This recognition has led to interest in constructing a model, for either on-line control or off-line optimization. through the simulation of the plant units on a digital or analog computer. If one keeps in mind the final objective of relating the plant output variables to the control variables, a computer simulation becomes a valuable aid in gaining an insight into the behavior of a plant unit, as well as in obtaining "operating experience" for systems engineers on the plant via the model. Simulation on a computer is certainly a more economical way to obtain data for a mathematical model of the plant than is experimentation on either a pilot plant or an actual plant.

The simulation model does not have to replicate the details of the entire process to be successful. The only requirement is that the model relate mathematically the process input variables to the process output variables in a reasonable manner, so that extrapolation beyond existing experimental data can be handled with confidence. The model can then be used to determine the optimum mode of operation for the actual plant, and the plant variables can be manipulated in the direction indicated by the experiments on the model.

This paper is the second in a series of simulation

studies^{1,2} in the petrochemical industry. These studies have been initiated to determine the problems involved in process control in this industry and to obtain simplified models for control and optimization studies of particular plant units, based on the physical and chemical phenomena taking place in these units. Simulation of a reactor for styrene production is treated here.

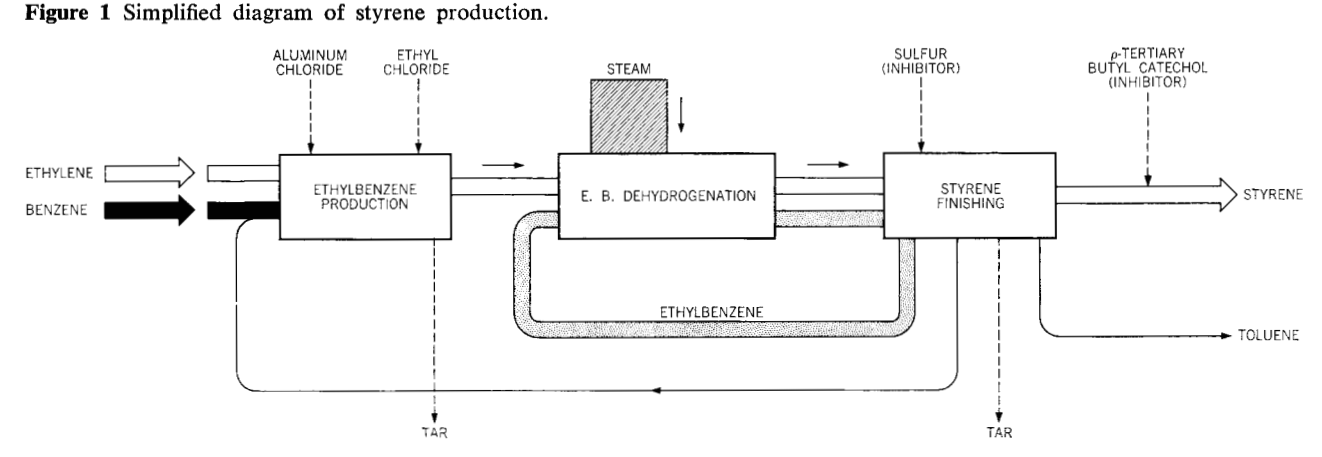
Styrene process

Three essential steps are associated with the production of styrene from benzene and ethylene:

- 1. synthesis of ethylbenzene from benzene and ethylene,
- 2. ethylbenzene dehydrogenation, and
- styrene finishing.

The three steps are coupled together by recycle streams and purification units. Figure 1 shows a simplified flow diagram of the process. A typical plant has a production capacity of about 100 million pounds per year. Although the first step in making ethylbenzene yields almost quantitative conversion (95 to 97%) due to recycling, the production costs could be reduced by improving the conversion per pass through the reactor and reducing the recycle rate. However, an even greater economic incentive lies in improved control of the conversion of ethylbenzene to styrene, a catalytic dehydrogenation process occurring in a fixed-bed reactor. It is possible to show that even a 1% gain in production can justify a small computer control system that will optimize the styrene manufacturing process. Furthermore, it has been shown that a computer control system often brings about the so-called unexpected or hidden gains by way of better scheduling and monitoring of the process.

Figure 2 shows the numerous units and recycle streams associated with the three essential process steps.



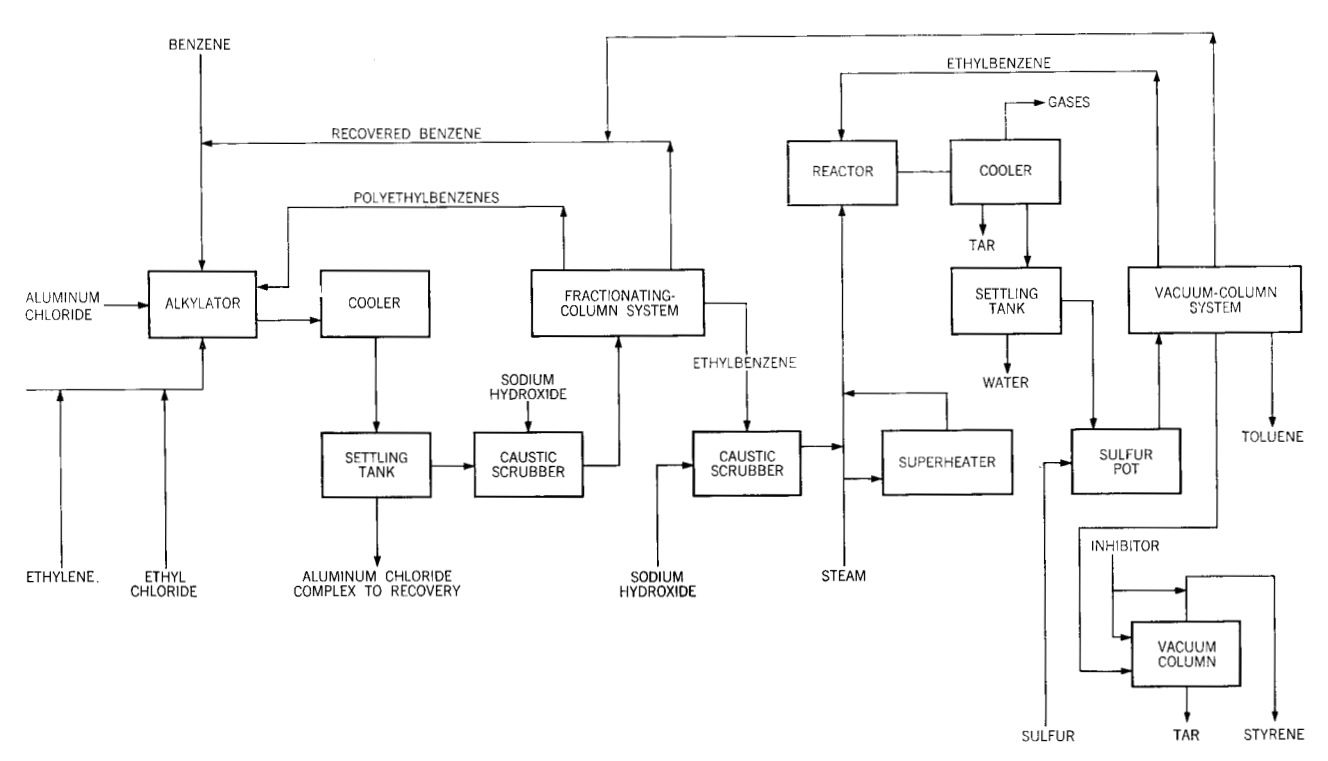


Figure 2 Flow diagram of styrene production.

Ethylbenzene is produced in the first step according to the following Friedel-Crafts reaction:

$$+ H_2C = CH_2 \xrightarrow{AlCl_3} CH_2 - CH_3$$

Side reactions also attach more ethylene molecules to the benzene ring, giving rise to polyethylates.

In the second step the ethylbenzene is catalytically dehydrogenated to styrene:

together with some other side reactions.

Representative yields for the over-all process are given in Table 1.

It is apparent that the yield obtained in Step 2 (90.1%) is the lowest of the three essential steps. This indicates that a closer approach to optimum operating conditions could show significant increases in the yield of crude styrene from ethylbenzene. Taking a production rate of 100 million pounds of styrene a year from ethylbenzene cracking as a basis, an increased yield in the conversion of ethylbenzene to styrene ($12\psi/lb$) of just 1% would

result in an increase of nearly \$100,000 in revenue per year. The efficiency in the conversion of benzene to ethylbenzene is perhaps the highest that can be achieved practically. It is difficult to justify a computer control system for ethylation based purely on the savings that might be achieved in the cost of recycling by increasing conversion per pass through the reactor. It is possible, though, that the increase in conversion might lead to higher total production. In any case, little is known about the kinetics and the mechanism of the Friedel-Crafts reaction of ethylbenzene synthesis.⁴

The simulation problem for the alkylator is further

Table 1 Over-all yields in the various steps of styrene production.⁴

Reactant	Product	Yield	
benzene	ethylbenzene	95.5%	
ethylene	ethylbenzene	96.8	
ethylbenzene	crude styrene	90.1	
crude styrene	finished styrene	99.4	

aggravated by the presence of many polyethylbenzenes differing in degrees of ethylation. Mathematical expressions for the reactor system become very involved because of the presence of three phases (solid catalyst, liquid benzene, ethylbenzene and gaseous ethylene) and various recycle streams. The kinetics of catalytic cracking of ethylbenzene to styrene, on the other hand, are better known and the simulation for the reactor is to some extent simpler than for the alkylator. In view of the higher economical incentive and the simplicity, this investigation was aimed at developing a mathematical model for the conversion of ethylbenzene to styrene.

Ethylbenzene/styrene conversion

• Dehydrogenation of ethylbenzene⁵

Figure 3 shows a cross-sectional view of a typical ethylbenzene dehydrogenation reactor.

Purified ethylbenzene, from the alkylation step, is preheated with steam to approximately 160°C. Superheated steam is then added to this mixture and fed continuously to the reactor. The final ratio of steam to ethylbenzene is about 2.6 to 1 by weight. The reactor is a fixed-bed type containing a selective dehydrogenation catalyst. The reaction products leave the top of the reactor at about 565°C, the major reactions being endothermic. The products are cooled first by the incoming ethylbenzene and then by steam in heat exchangers. A spray-type cooler lowers the product temperature to about 105°C, and condenses out tars. A final condenser liquifies the steam, styrene monomer, toluene, and benzene, while the vent gases go to a refrigeration recovery system. The condensed materials pass to a settling tank, where the hydrocarbons are decanted and the water is discharged to a disposal system.

• Thermodynamics of ethylbenzene cracking

The primary chemical reaction in the dehydrogenation of ethylbenzene is

$$C_6H_5 - C_2H_5 \Leftrightarrow C_6H_5 - CH = CH_2 + H_2$$
.

The reaction is endothermic and the true equilibrium constant K_a , based on the activities, increases as temperature increases in accordance with van't Hoff's law.

For ideal gas behavior in the reactor, K_a can be expressed by

$$K_{a}(T) = \frac{N_{\rm S} N_{\rm H_{2}} \cdot \pi}{N_{\rm E.B.} N_{\rm total}}$$

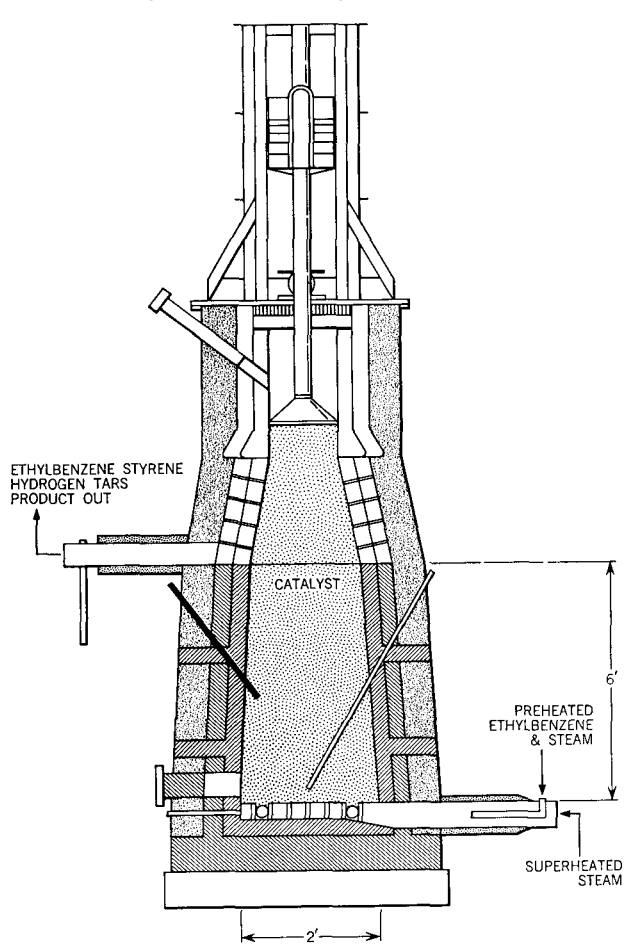
$$= \frac{N_{\rm S} N_{\rm H_{2}} \cdot \pi}{N_{\rm E.B.} (N_{\rm S} + N_{\rm E.B.} + N_{\rm H_{2}} + N_{\rm I})}, \qquad (1)$$

where the subscripts S, E.B., and I refer respectively to styrene, ethylbenzene, and inert gas. Since K_a is only a

function of temperature, increase in styrene yield (N_s) can only be achieved by operating at low pressures or by increasing the number of inert molecules. Thus, either steam or benzene as an inert in the ratio of 2.6 lbs/lb of ethylbenzene is fed to the reactor to reduce the partial pressure of reaction products to about 0.1 atm in the total operating pressure of about 1.2 to 1.4 atm. It is found that with no inert, the equilibrium conversion is only about 25 to 30% at 630°C, whereas with the steam supplied in the ratio indicated above the equilibrium is raised to 80 to 85%.

Although the reaction rate of styrene formation is rapid at 700°C, undesirable side cracking reactions produce large amounts of toluene and benzene at this temperature.⁴ However, with the use of selective dehydrogenation catalysts such as SnO, Cr₂O₃, FeO, MgO, activated charcoal, alumina or bauxites, rapid formation of styrene is obtained, even at low temperatures, minimizing the side reactions.

Figure 3 Ethylbenzene dehydrogenation reactor.



• Chemistry of ethylbenzene cracking⁴

In spite of selective dehydrogenation catalysts, small quantities of CO, CO₂, CH₄, H₂, C₆H₆, toluene, C₂H₄, and C₂H₂, along with carbon, are present in the effluent stream from the reactor. A typical effluent has 37% styrene, 61% ethylbenzene, 1.4% toluene, 0.6% benzene (by weight), and traces of C₂H₄, C₂H₂, CO, CO₂, and H₂. Carbon is present in small amounts as coke.

The steady-state operation of the styrene reactor can be described, once the various chemical reactions that give rise to the products observed in the reactor effluent are known. In general, the exact mechanism that can explain the formations of the products is subject to discussion. For our purpose, it is sufficient to postulate some plausible and consistent set of chemical events that account for all the chemical species in the product. Thus, the following events are postulated to describe the reactions in the dehydrogenation of ethylbenzene:

- 1) $C_6H_5C_2H_5 \Leftrightarrow C_6H_5C_2H_3 + H_2$ catalytic
- 2) $C_6H_5C_2H_5 \rightarrow C_6H_6 + C_2H_4$ catalytic
- 3) $H_2 + C_6H_5C_2H_5 \rightarrow C_6H_5CH_3 + CH_4$ catalytic
- 4) $CH_4 + H_2O \rightarrow CO + 3H_2$ catalytic
- 5) $CO + H_2O \rightarrow CO_2 + H_2$ catalytic
- 6) $C_2H_4 \rightarrow C_2H_2 + H_2$ vapor phase thermal cracking
- 7) $C_2H_2 \rightarrow 2C + H_2$ vapor phase thermal cracking
- 8) $C + 2H_2O \rightarrow CO_2 + 2H_2$

solid carbon deposited on catalyst

The eight events occur simultaneously, yielding the observed products. Events 1 through 5 are postulated as being surface catalyzed and controlled heterogeneous reactions. It is assumed that the catalyst promotes these reactions without interactions between the reactions on the surface. This implies that Event 1 occurs as if Events 2 through 5 are not present. Events 6 and 7 are presumed to be homogeneous reactions. It is entirely possible that the dehydrogenation catalyst also catalyzes the cracking of ethylene and acetylene, but this mechanism only complicates the over-all objective without contributing substantially to the steady-state description of the system.

• Kinetics of ethylbenzene cracking

Four kinetic studies on the catalytic cracking of ethylbenzene by Rase and Kirk⁶, Wenner and Dybdal⁷, Shuikin and Levitsky^{7a} and Carra and Forni^{7b} are found in the literature. Rate equations based on Events 1 through 3 by Wenner and Dybdal⁷ are used in our simulation.

For Event 1, the rate of styrene production r_{10} is given by

Event
$$l r_{10} = k_{10}[p_9 - p_{10}p_{11}/K_p].$$
 (2)

The dependence of k on temperature is given by

$$k_{10}(T) = \exp\left[-5715/T - 6.16\right].$$
 (3)

The equilibrium constant is also a function of temperature and according to the van't Hoff equation

$$d(\ln K_p)/dT = \Delta H^{\circ}/RT^2. \tag{4}$$

The values of ΔH° are given by Wenner and Dybdal⁷ as 29,715 at 800°K and 29,824 at 900°K. A simple linear dependence on temperature within this range can be constructed as

$$\Delta H^{\circ} = 28,843 + 1.09T. \tag{5}$$

Integration of Eq. (4) subject to the condition that $K_p = 1.00$ at 956°K^7 yields the following relationship:

$$K_p = (T)^{0.549} \exp \left[-14516/T + 11.41\right].$$
 (6)

In the operating range of 525° to 650° C, the equilibrium constant K_{p} in Eq. (6) is orders of magnitude smaller than the K_{p} values in Events 2 and 3, so that the reverse reactions can be neglected in these two events. The corresponding rate equations are:

Event 2
$$r_{12} = \exp\left[-25600/T + 12.8\right]p_9;$$
 (7)

Event 3
$$r_{14} = \exp \left[-11000/T - 1.8\right] p_9 p_{11}$$
. (8)

The rate expression of the methane-steam reaction over a reduced nickel catalyst, supported on kieselguhr cylindrical pellets, was determined by Akers and Camp⁸ as

Event 4
$$r_{16} = \exp[-7900/T - 3.36]p_{15}$$
. (9)

The carbon monoxide - steam reaction rate over a promoted iron oxide catalyst can be expressed by 9

Event 5
$$r_{18} = \frac{\pi}{T^3} \exp\left[-8850/T + 3.80\right] \vec{p}_{18} p_{17}.$$
 (10)

The homogeneous gas phase irreversible cracking of ethylene is described by 10

Event 6
$$r_{19} = 2.15 \times 10^{11}$$

 $\times (1/T) \exp \left[-38000/T\right] p_{13}, (11)$

and the homogeneous gas phase irreversible cracking of acetylene is expressed by⁷

Event 7
$$r_{11} = 1.18 \times 10^{9}$$

 $\times (1/T) \exp \left[-30950/T|p_{19}\right]. (12)$

The kinetic expression for steam-carbon reaction below 700°C is given by¹¹

Event 8
$$r_{17} = 1.11 \times 10^5$$

$$\times \exp \left[-34000/T\right](p_{17})^2$$
. (13)

Reactions in Events 4 through 8 are found to be negligible.

It will be assumed that the literature data for the above

rate equations are substantially correct, at least in the orders of magnitude of the Arrhenius constant.

When simulating the conversion of ethylbenzene in Event 1, it is possible that mathematically X_1 , the fractional conversion, might exceed the value predicted by the thermodynamic equilibrium value at a particular temperature and pressure. A restriction must be imposed to eliminate this difficulty. If one assumes that styrene is the only reaction product of ethylbenzene, and if $Y_1 = \text{gm}$ moles of ethylbenzene converted at equilibrium per gm mole of ethylbenzene, in the feed, and $r = N_s/F$, then at equilibrium

Moles of ethylbenzene
$$n_9 = F(1 - Y_1)$$

Moles of styrene $n_{10} = FY_1$
Moles of H_2 $n_{11} = FY_1$
Moles of steam $n_{17} = N_s$
Total moles $n_t = F(1 + Y_1 + r)$. (14)

Now

$$K_p = p_{10}p_{11}p_9 = \frac{Y_1^2\pi}{(1-Y_1)(1+Y_1+r)};$$
 (15)

so tha

$$Y_1 = \frac{r + \sqrt{r^2 + 4(1 + \pi/K_p)(1 + r)}}{2(1 + \pi/K_p)}, \qquad (16)$$

where K_p is given by Eq. (6).

Since X_1 , the conversion of ethylbenzene in Event 1, must always be less than or equal to the equilibrium value given by Eq. (16), the following limitation is imposed in the program:

$$X_1 \le Y_1$$
 for all values of T and r . (17)

Heats of reaction and heat capacities

· Heats of reaction

The standard heat of reaction ΔH° over our limited temperature range of interest (527° to 627°C) can be represented by a linear dependence on temperature. Table 2 shows ΔH° values given by Wenner and Dybdal⁷ used for this purpose.

The ΔH° relationships for Events 6 through 8 may be written from specific heat data as

$$\Delta H^{\circ} = \Delta H_{\circ} + \Delta \alpha T + (\Delta \beta / 2) T^{2} + (\Delta \gamma / 3) T^{3} + \cdots, \qquad (18)$$

which is the general relationship for the temperature dependence of the standard heat of reaction. An error of less than 5% is encountered if Eq. (18) is truncated after the linear term.

The quantity $\Delta \alpha$ was determined from tables of standard

Table 2 Heats of reaction for various events.

Event	Heats of reaction (ΔH°)
1	28,843 + 1.09 T
2	25,992 - 1.90 T
3	12,702 - 3.15 T
4	50,046 + 3.96 T
5	10,802 + 2.5 T
6	38,278 + 11.45 T
7	-56,524 + 7.82 T
8	22,320 - 2.604 T

heat of reaction data at 25°C and heat capacity data, respectively.¹²

• Heat capacities

The equations for C_p^0 of ethylbenzene and styrene were derived from the tabulated values⁴ for 800° K and 900° K.

Ethylbenzene:
$$C_{p_s}^0 = 34.4 + 0.041 T$$

Styrene: $C_{p_{10}}^0 = 33.16 + 0.0353 T$. (19)

For the rest of the compounds, since they appear in small quantities, similar linear heat capacity equations were derived from the data of Smith¹² for our temperature range of 527° to 627°C.

Calculation of molar concentrations

If X_i represents the conversion of the reactant in i^{th} reaction, the respective moles/sec at any point in the reactor in the gaseous phase are given by:

Ethylhomaono	$n_0 = F(1 - X_1 - X_2 - X_3),$
Ethylbenzene	$n_9 = \Gamma(1 - \lambda_1 - \lambda_2 - \lambda_3),$
Styrene	$n_{10}=FX_1,$
Hydrogen	$n_{11} = F(X_1 - X_3 + X_6 + X_7) +$
	$N_s(3X_4+X_5+X_8),$
Benzene	$n_{12}=FX_2,$
Ethylene	$n_{13} = F(X_2 - X_6),$
Toluene	$n_{14}=FX_3,$
Methane	$n_{15} = FX_3 - N_s X_4, (20)$
Carbon monoxide	$n_{16} = N_s(X_4 - X_5),$
Steam	$n_{17} = N_s(1 - X_4 - X_5 - X_8),$
Carbon dioxide	$n_{18} = N_s(X_5 + \frac{1}{2}X_8),$
Acetylene	$n_{19} = F(X_6 - X_7).$

Thus, the total moles in the gas phase are

$$n_t = F(1 + X_1 + X_2 + X_6) + N_s(1 + 3X_4 + \frac{1}{2}X_8).$$
 (21)

The number of moles of coke produced is given by

$$n_{20} = F(2X_7) - N_s(\frac{1}{2}X_8). \tag{22}$$

Assuming ideal gas behavior for our low pressure

reactor, the partial pressures can be written in terms of conversions by combining

$$p_i = (n_i/n_t)\pi, (23)$$

and Eqs. (20) and (21).

Pressure loss through the reactor

Hougen and Watson¹³ have given an expression for pressure drop through randomly packed beds. It was found however, with the use of this expression and typical reactor conditions, that the resulting pressure drop can be simply and adequately described by a parabolic expression:

$$\pi - 1 = C \times 10^{-6} (z - 1000)^2, \tag{24}$$

which is valid for 0 < z < 1000 cm. The value of constant C depends on $\pi(0)$ and can be calculated by

$$C = [\pi(0) - 1]. (25)$$

The details of the procedure for arriving at Eq. (24) may be found elsewhere.¹⁴

Material and energy balances

Having assembled all the thermodynamic and kinetic data, we are now ready to write the material balance equations. The material balance for a small section of the reactor is expressed, with the aid of kinetic expressions and pressure drop formulations in the sections on Kinetics of Ethylbenzene Cracking, and Simplifications of Rate Expressions, respectively, as follows:

Event 1:
$$F\frac{dX_1}{dz} = r_{10}\alpha\delta\rho_w, \qquad (26)$$

Event 2:
$$F\frac{dX_2}{d\tau} = r_{12}\alpha\delta\rho_w, \qquad (27)$$

Event 3:
$$F\frac{dX_3}{dz} = r_{14}\alpha\delta\rho_w, \qquad (28)$$

Event 4:
$$F\frac{dX_4}{dz} = r_{16}\alpha\delta\rho_w, \qquad (29)$$

Event 5:
$$N_* \frac{dX_5}{dz} = r_{18} \alpha \delta \rho_w, \qquad (30)$$

Event 6:
$$F\frac{dX_6}{dz} = r_{19}\alpha(1 - \delta),$$
 (31)

Event 7:
$$F\frac{dX_7}{dz} = r_{11}\alpha(1 - \delta),$$
 (32)

Event 8:
$$N_s \frac{dX_8}{dz} = r_{17}\alpha(1-\delta),$$
 (33)

where the r_i 's are given in Eqs. (2) and (7) through (13),

and the p_i 's are obtained by combining Eqs. (20), (21), and (23).*

The X_i 's represent fractional conversion in i^{th} event, α is the cross section area of the reactor, δ is the ratio of the volume of catalyst pellets to the reactor volume, and ρ_w is the bulk density of catalyst pellets.

• Energy balance

For the reactor section of height dz, the energy balance is

$$-F \sum \frac{dX_i}{dz} \Delta H_i^0(T) - N_s \sum \frac{dX_i}{dz} \Delta H_i^0$$
$$- U(T - T_s) \frac{4\alpha}{D} = \sum n_i C_{\nu_i}^0 \frac{dT}{dz}, \qquad (34)$$

where the first summation on the left-hand side of the equation is over Events 1, 2, 3, 5, and 6; the second summation is over Events 4, 5, and 8; and the summation on the right-hand side is for all components present in the gaseous phase. The terms ΔH_i and C_{p_i} are all functions of temperature, and the formulations from the section on Heats of Reaction and Heat Capacities can be substituted in Eq. (34) to complete the energy balance.

Initial runs indicated that Events 4 through 8 produced small quantities of products, so that for all practical purposes the left-hand side of Eq. (34) will reduce to

$$-F \sum_{i=1}^{3} \frac{dX_{i}}{dz} \Delta H_{i}^{0}(T) - U(T - T_{\bullet}) \frac{4\alpha}{D}$$

$$= \sum_{i=1}^{3} n_{i} C_{pi}^{0} \frac{dT}{dz}, \qquad (35)^{\dagger}$$

with the summation on the right-hand side to be taken over the components involved in the first three events and steam.

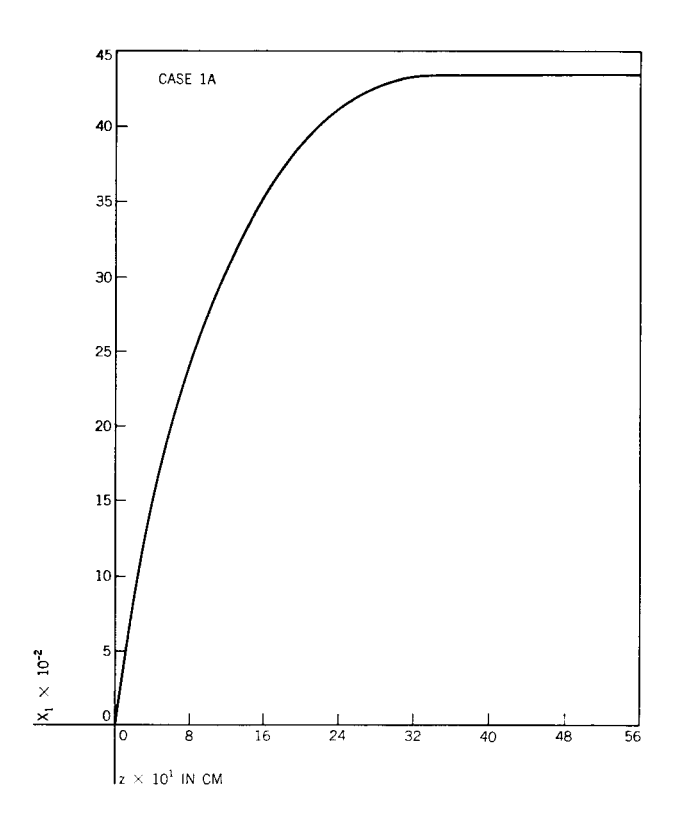
The boundary conditions for Eqs. (26) through (35) are: at z=0, $X_i=0$, $T=T_0$. The nine coupled differential equations need to be solved to determine product composition at the reactor exit. It is also of interest to find the effect of the various parameters in the equations on the exit composition and styrene production. These equations were solved by using a fourth-order Runge-Kutta integration technique with an IBM 7090 computer program. The program description and FORTRAN listing are given elsewhere.¹⁴

Discussion of results

Figure 4 shows plots of conversion of ethylbenzene to

[•] We have neglected the radial gradients, and assumed that their effect on the over-all reactor output will be small. For an insulated adiabatic reactor this assumption does not incur serious errors.

[†] The pressure-flow work term is small and can be neglected without disturbing the general picture. Potential and kinetic energy terms are also small and are neglected.



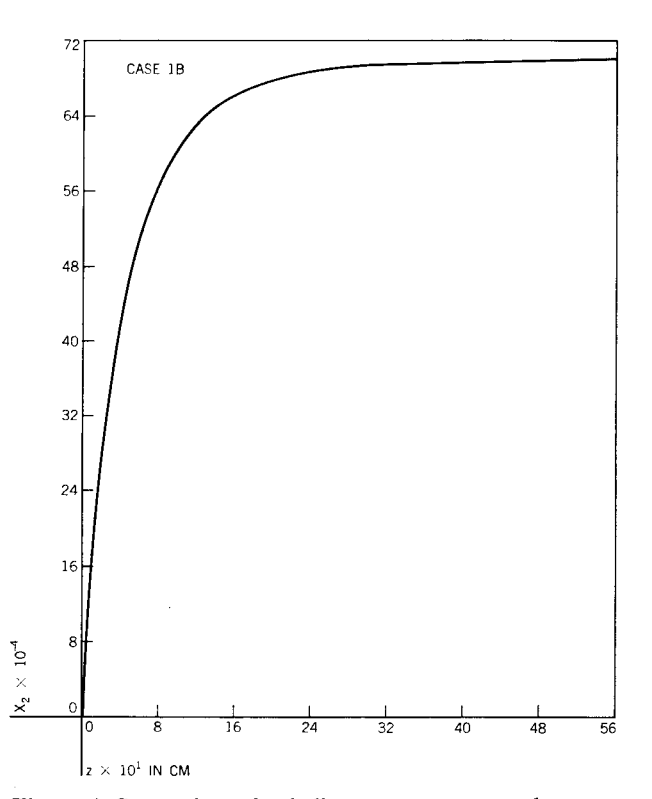
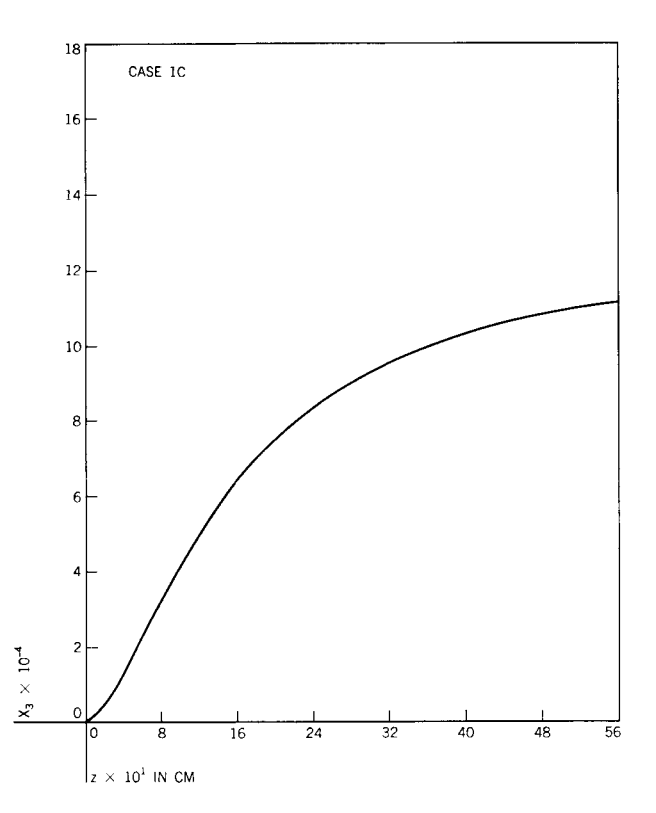


Figure 4 Conversion of ethylbenzene to styrene, benzene, and toluene along the reactor bed depth.



styrene X_1 , to benzene X_2 , and to toluene X_3 as a function of catalyst bed depth for typical conditions of feed, feed temperature and steam/feed ratio. Figure 5 shows plots of the temperature of the reaction mixture versus bed depth for the same conditions. As we would expect in a process with a major endothermic reaction, the temperature drops along the reactor length and the conversion to styrene rises rapidly initially and reaches equilibrium toward the reactor exit. The benzene formation follows the same trend whereas the toluene formation is slower, since H2 is required for this reaction from subsequent reactions. The equilibrium styrene conversion (which is never exceeded in the reactor) follows the same trend as the temperature (Fig. 6). These results agree very well with the data of Wenner and Dybdal. Also, the carbon formation X_7 is very small and, due to the preponderance of steam, very little residual carbon is deposited on the catalyst, at least for the reactor conditions listed on these figures. (See Table 3.)

It is of interest next to determine the effect of feed rate, steam/feed ratio, temperature of the mixture at the reactor inlet, pressure at the entrance to the reactor, and the over-all heat transfer coefficient on the reactor performance, as well as yield of styrene. The computer

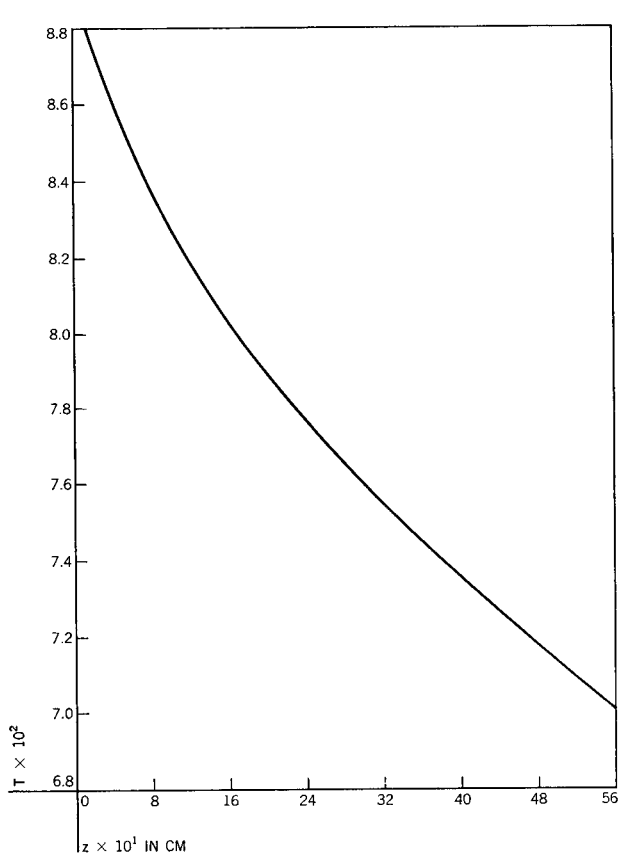


Figure 5 Temperature of the reaction mixture in the reactor.

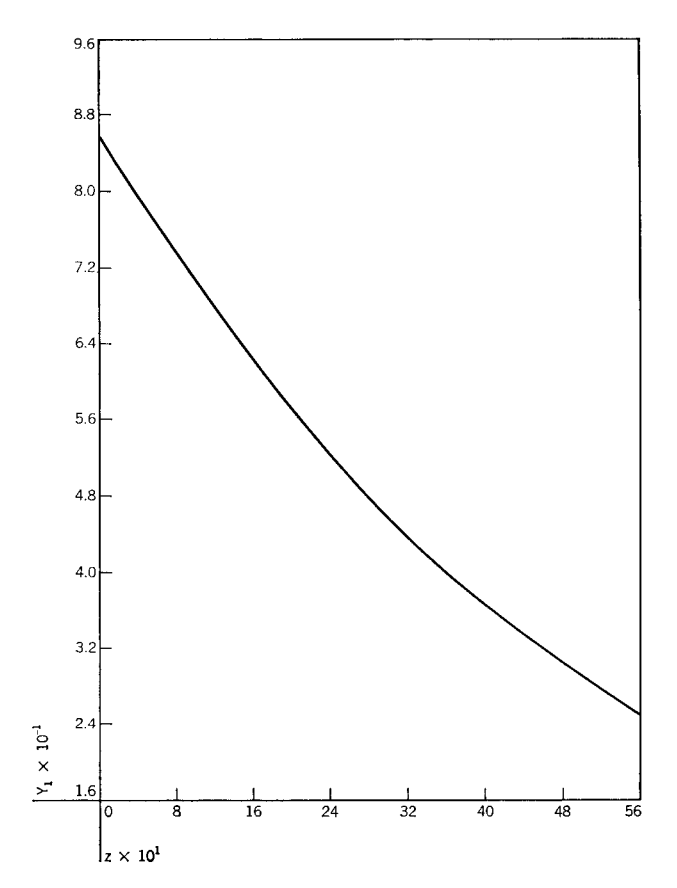


Figure 6 Equilibrium conversion along the reactor depth.

program was, therefore, run for several values of these variables to ascertain their effects. The various parameters used in these runs are tabulated in Table 3.

Since one of the main purposes of this study is to find optimum profit from the styrene production, we will examine next the results of the various runs where the parameters listed in Table 3 were varied. The yield of styrene is directly proportional to plant profit, and for this reason we have calculated styrene conversion at the reactor exit as a function of the various parameters. The actual profit function will include penalty for benzene and toluene, purification costs, and increase or decrease in down time due to increased or decreased coking.

• Effect of variation in heat transfer coefficient U

Figure 7 illustrates a plot of the temperature along the reactor length for various values of U, and Fig. 8 shows the effect of U on the styrene conversion. As we would expect, an adiabatic reaction (U=0) is the ideal situation. The conversion, and hence the yield, drops by about 20% when U increases from 17×10^{-5} to 60×10^{-5} cal/sec cm² °C. Thus, in a poorly insulated reactor, the

Figure 7 Plot of mean bed temperature versus axial distance for various values of U.

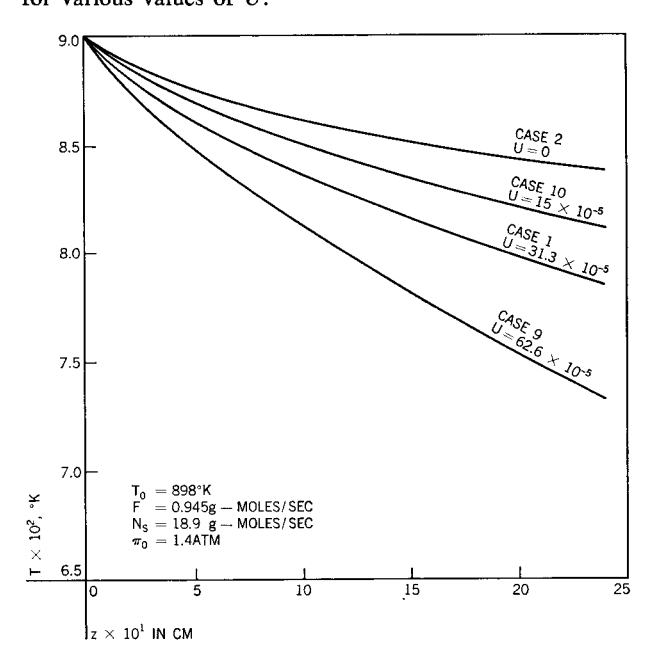


Table 3 Computer runs for various parameter values.

Run No.	π_0	F	N_s	r	$U \times 10^{+5}$	T_0
1	1.4	0.945	18.9	20.0	31.3	898
2	1.4	0.945	18.9	20.0	0.0	898
3	1.4	0.945	18.9	20.0	31.3	913
4	1.4	0.945	18.9	20.0	31.3	923
5	1.4	0.945	18.9	20.0	31.3	883
6	1.4	1.134	18.9	16.667	31.3	898
7	1.4	1.0395	18.9	18.182	31.3	898
8	1.4	0.8505	18.9	22.222	31.3	898
9	1.4	0.945	18.9	20.0	62.6	898
10	1.4	0.945	18.9	20.0	15.0	898
11	1.6	0.945	18.9	20.0	31.3	898
12	1.8	0.945	18.9	20.0	31.3	898
13	1.2	0.945	18.9	20.0	31.3	898
14	1.4	18.9	0.945	0.05	0.0	898

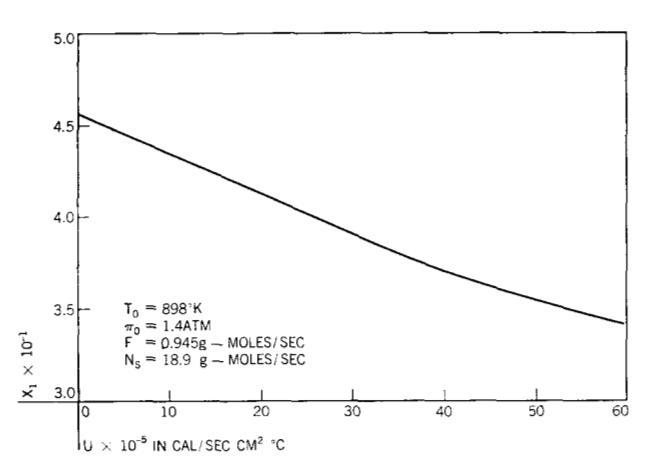
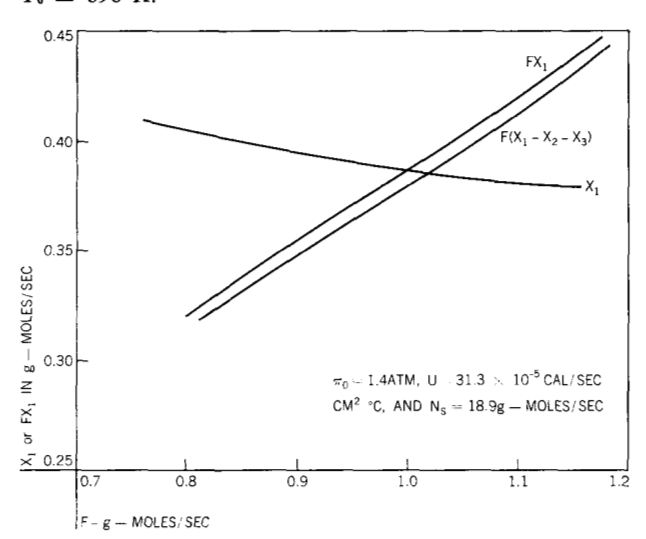


Figure 8 Plot of ethylbenzene conversion in Event 1 at z = 200 cm vs U.

Figure 9 Plots of X_1 and FX_1 vs F at z=200 cm with $T_0=898$ °K.



conversion can vary considerably with wind velocity and ambient conditions such as rain, sun, etc. The need for insulating the reactor well is then apparent if we are striving for high styrene yields.

• Feed rate F

When the feed rate of ethylbenzene is increased while keeping the steam rate constant, the conversion to styrene drops slightly as shown in Fig. 9. However, if the total styrene yield, and hence the actual profit relation, is expressed by $F(X_1 - W_2X_2 - W_3X_3)$, where W_2 and W_3 are weighting factors for separation costs, we see that the profit curve increases monotonically with increasing F. There will be, of course, limiting flow conditions due not only to increased pressure drop through the reactor, but also to catalyst loss in the exit stream and capacity restrictions of subsequent separating units.

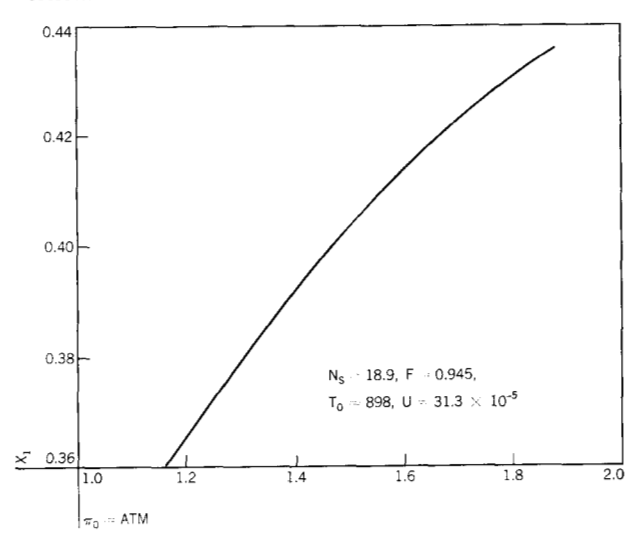
• Inlet pressure π_0

Figure 10 shows the effect of variation in inlet pressure on the conversion of styrene. Here again the conversion goes up almost linearly with the inlet pressure in the range examined. However, the equilibrium conversion of styrene is inversely proportional to the pressure. Also, the reverse reaction as indicated in Eq. (26) is proportional to π^2 , whereas the forward reaction of styrene formation is proportional to π . Thus, we see in Fig. 11 that, beyond a certain limit, an increase in π_0 will cease to increase conversion of ethylbenzene to styrene.

• Inlet temperature T₀

Figure 12 depicts the effect of an increase in feed temperature on styrene conversion. Again in the 40°C temperature

Figure 10 Effect of inlet pressure variation on styrene conversion.



range examined, styrene formation increases linearly. Notice, though, in Table 4 that the carbon deposition rate X_7 increases 75-fold when temperature is increased by 40°C. Thus, if we were to include in the profit function a down time penalty for coking, the profit would show an optimum when plotted against T_0 . It is known that due to coking and other side reactions, the catalyst activity decreases over a period of one year. Thus, to maintain a steady styrene production, the feed temperature has to be increased to compensate the decline in activity. Normally, a 30°C increase over a year is sufficient for this purpose.⁴

• Steam-to-feed ratio

Figure 9 showed how an increase in feed F, keeping the steam rate N_s constant, decreases conversion X_1 . Run No. 14 deals with the situation when U = 0 and the ratio $N_s/F = r$ is reduced drastically to 0.05, keeping the total molal feed rate the same as when r = 20. When we compare the results of runs 2 and 14, we see that reduction of r reduced the conversion by 53%, although total styrene production increased tenfold. The decrease in values of X_1 and Y_1 is due to the reasons pointed out in the section on Thermodynamics of Ethylbenzene Cracking. It appears, then, that the optimum steam/feed ratio will depend upon the penalty function for coking, the cost of separating the various products, and the cost of preheating ethylbenzene indirectly, to raise it to the required temperature-especially in cases where a very low value of r is used. If heating is only to be accomplished by superheated steam, the ratio may be limited by the maximum temperature at which the superheated steam is available.

• Simplified model for control

It is obvious that the mathematical model presented here is unsuitable for use on a process control computer either for off-time optimization or on-time control. Based on the simulation results discussed here, however, a simple model may be derived for the smaller computer. Our results indicate that the yield of styrene, FX_1 , is linearly proportional to F and π_0 . It varies with U and T_0 in a quadratic fashion. Since the penalty for coking and separation costs also increase with the increase in temperature and yield of byproducts, the profit function based purely on styrene yield would have the following form:

Profit =
$$C_1 F X_1 = C_2 + C_3 F$$

 $+ C_4 \pi_0 + C_5 U(T_s) + C_6 U^2(T_s)$
 $+ C_7 T_0 + C_8 T_0^2 - C_9 f(T_0)$
 $- C_{10} X_1 - (C_{11} r + C_{12} r^2),$ (36)

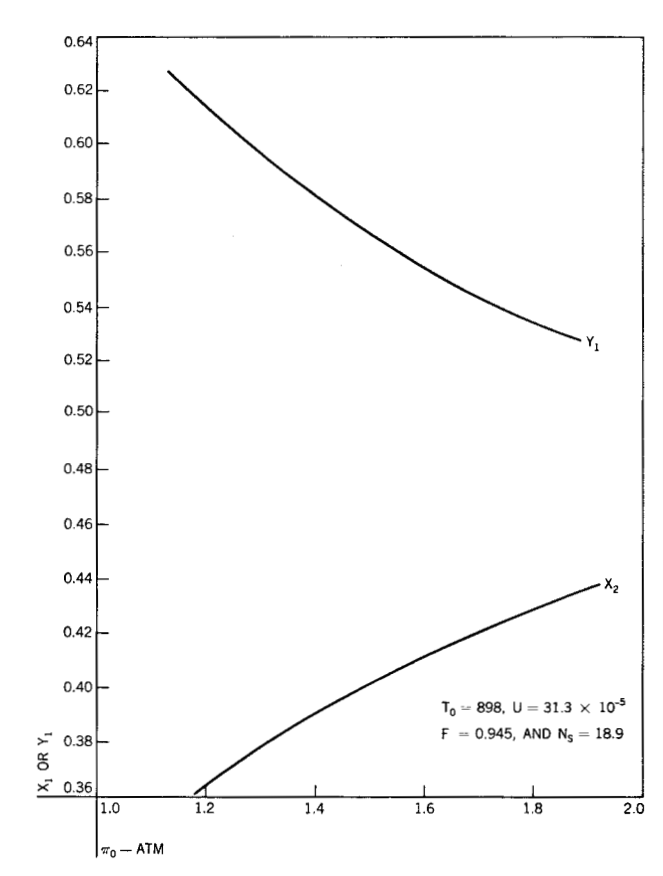
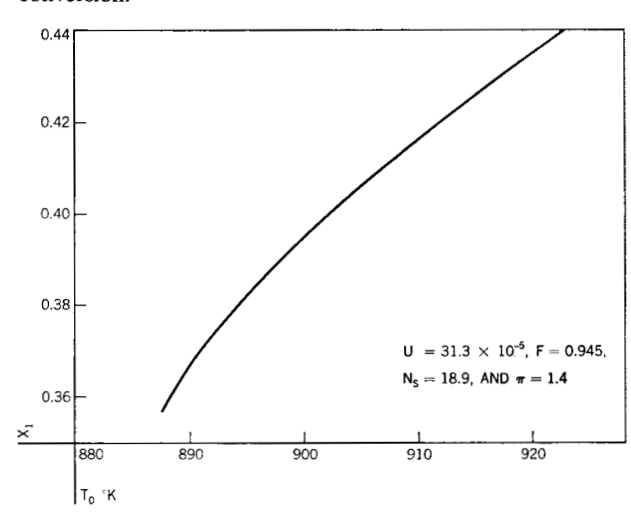


Figure 11 Opposing effect of inlet pressure on equilibrium conversion and actual conversion.

Figure 12 Effect of increase in inlet temperature on styrene conversion.



where the constants are to be interpreted as follows:

 C_1 refers to cost of styrene

C2 includes raw material cost and fixed costs

 C^3 is obtained by making use of Fig. 9

Table 4 Numerical results at z = 200 cm.

Case No.	T	Y_1	X_1	$\begin{matrix} X_2 \\ (\times 10^3) \end{matrix}$	$\begin{array}{c} X_3 \\ (\times 10^4) \end{array}$	$(\times 10^6)$	$(\times 10^{12})$	$(\times 10^9)$	$\begin{array}{c} X_7 \\ (\times 10^{14}) \end{array}$	$(\times 10^{15})$
1	797	0.582	0.391	6.78	7.53	8,66	1.96	2.99	2.24	4.48
2	844	0.754	0.453	10.45	11.53	15.96	4.25	8.87	11.11	22.22
3	808	0.624	0.420	10.40	9.48	12.3	3.13	8.79	11.10	22.20
4	814	0.651	0.440	13.6	10.95	15.3	4.22	17.6	31.2	62.4
5	786	0.539	0.362	4.36	5.90	5.98	1.20	0.976	0.425	0.849
6	795	0.545	0.380	6.47	8.47	11.4	2.48	2.67	1.89	4.54
7	796	0.563	0.385	6.62	8.02	10.0	2.22	2.82	2.05	4.51
8	798	0.604	0.397	6.96	7.02	7.37	1.71	3.19	2.46	4.43
9	753	0.403	0.338	4.94	5.05	4.88	0.946	1.47	0.763	1.53
10	821	0,676	0.423	8.35	9.38	11.9	2.92	4.95	4.73	9.46
11	795	0.556	0.412	7.17	9.69	12.2	3.87	3.37	2.69	5.39
12	793	0.533	0.429	7.52	12.1	16.6	7.10	3.72	3.16	6.32
13	800	0.612	0.365	6.34	5.63	5.8	0.902	2.59	1.79	3.58
14	807	0.216	0.211	4.08	71.4	27,019.0	203.0	0.830	0.340	272.0

 C_4 is obtained from Fig. 10

 C_5 and C_6 are obtained from Fig. 7

 C_7 and C_8 are obtained from Fig. 12

 C_9 and f are obtained from the penalty function of coking to be specified. The function f may be exponential.

 C_{10} refers to cost of separation

 C_{11} and C_{12} may be introduced and calculated from our results if the steam source fluctuates heavily.

The constant C_2 will also include the first constant term obtained from each curve when linear or quadratic relationships are obtained from the curves.

It is not the purpose of this paper to derive a profit function for a particular plant by determining the constants C_1 through C_{12} . Each plant may have its own constraint on the profit function which differs from other plants. The way to obtain this function is to recalculate the simulation results for a particular plant and after a reliable fit is obtained between the results and the plant measurement, the constants in Eq. (36) can be determined for the plant for the range of variation in F, r, T_0 , T_0 and π_0 permitted by the plant constraints. The next step of optimization and on-time control calculations may then be performed with Eq. (36) within the specified constraints on the plant variables.

Acknowledgment

The authors are grateful to Keith Johnson for writing the computer programs and carrying out the numerical computations.

References

- M. J. Shah, "Simulation of a Thermal Cracking Furnace," to be presented at the 56th AlChE National Meeting, San Francisco, May 1965.
- M. J. Shah, Chester James, and J. H. Duffin, "Simulation of an Ammonia Synthesis Reactor," paper to be presented at the 1966 IFAC Conference.
- 3. D. B. Brandon, I and EC, 52, No. 10, 815 (1960).
- E. M. Marks, J. M. Almand, and E. E. Reid, J. Org. Chem. 9, 13 (1944).
- R. H. Boundy, and R. F. Boyer, Styrene, its Polymers, Copolymers and Derivatives, Reinhold Publishing Corp., New York, 1952.
- 6. H. F. Rase, and R. S. Kirk, CEP, 50, No. 1, 35 (1954).
- 7. R. R. Wenner, and E. C. Dybdal, *CEP* 44, No. 4, 275 (1948).
- N. I. Shuikin and I. I. Levitsky, *Bull. Acad. Sci.* No. 4, 592 (1952).
- S. Carra and L. Forni, *I and EC*, *Design and Devel.* 4, No. 3, 281-5 (1965).
- 8. W. W. Akers and O. P. Camp, *J. AIChE* 1, No. 4, 471, (1955).
- 9. A. A. O'Kelly, *I* and *EC*, **3**9, 154 (1947).
- G. D. Towell, "Kinetics of the Thermal Decomposition of Ethane to Acetylene in Non-Uniform Temperature Fields," Ph.D. Thesis, University of Michigan, 1961.
- 11. G. S. Scott, I and EC, 33, No. 10, 1279 (1941).
- J. M. Smith, Introduction to Chemical Engineering Thermodynamics, McGraw-Hill Book Co., Inc., New York, 1959.
- 13. O. A. Hougen, and K. M. Watson, *Chemical Process Principles*, Vol. III, p. 1017, Eq. 17, John Wiley and Sons, New York, 1962.
- 14. B. Davidson, and M. J. Shah, IBM Technical Report, TR 02.340, "Simulation of the Catalytic Cracking Process for Styrene Production," IBM Systems Development Division Laboratory, San Jose, California.

Received April 8, 1965.